Available online at www.sciencedirect.com
ScienceDirect
Trans. Nonferrous Met. Soc. China 31(2021) 2081−2101
Transactions of Nonferrous Metals Society of China
www.tnmsc.cn

Typical roles of metal ions in mineral flotation: A review

Zhi-yong GAO[1,2], Zhe-yi JIANG[1,2], Wei SUN[1,2], Yue-sheng GAO[3]

1. School of Minerals Processing and Bioengineering, Central South University, Changsha 410083, China;
2. Key Laboratory of Hunan Province for Clean and Efficient Utilization of Strategic Calcium-containing Mineral Resources, Central South University, Changsha 410083, China;
3. Department of Chemical Engineering, Michigan Technological University, Houghton 49931, United States

Received 24 July 2020; accepted 20 January 2021

Abstract: In flotation, metal ions possess significant roles that are usually fulfilled by either selectively activating or depressing the target minerals. Despite that tremendous efforts have been made to address the roles of metal ions in flotation, it still lacks a comprehensive review, especially to compare various ions instead of focusing on a specific one. This review begins by elaborately categorizing the factors involved in affecting the roles of metal ions in flotation. After that, well-accepted mechanisms are updated and discussed from the ore type. Furthermore, typical approaches to explore the underlying mechanisms are emphasized, including traditional techniques such as micro-flotation, contact angle measurement, zeta potential measurement, and other recent prevailing methodologies, like computational method, solution chemistry calculation, and cyclic voltammetry. This work will pave the way to promote flotations via activities like selectively adding/reducing metal ions, choosing reagents, and regulating the slurry chemistry.
Key words: metal ions; flotation; oxide mineral; silicate mineral; sulfide mineral

1 Introduction

Flotation is a versatile method extensively used in mineral processing fields to separate valuable minerals from gangue minerals selectively, which is based on the wettability differences among mineral surfaces [1,2]. Metal ions, mainly originated from grinding media, dissolution of minerals, and the use of the process water, etc, can make a substantial impact on the flotation. For instance, the presence of Ca^{2+} and Mg^{2+} takes different effects on flotations of galena, pyrite, and sphalerite [3−5]. Besides, it is hard to separate zircon from cassiterite when using fatty acid as a single collector, since both recoveries maintain relatively low levels. Nevertheless, zircon is proven to be selectively activated by Fe^{3+}, while cassiterite is not [6]. On the other hand, some inadvertent activations are harmful to the flotation separation. It is well known that some divalent ions, like Zn^{2+}, Pb^{2+} and Ni^{2+}, may accidentally activate quartz, leading to a low-quality concentrate product [7].

The effects of metal ions on flotations have been intensively reported since the 1950s [8]. However, the previous reports have mainly focused on the influence of a specific metal ion on the flotation of a particular mineral. Hence, there is still a lack of a systematic summary on topics such as categorizing the related factors, updating the latest understandings of the underlying mechanisms, as well as the research approaches. Specifically, the well-accepted mechanisms have been proposed for decades. They can be divided into two hypotheses, i.e., metal ion hydroxyl complexes [9] and adsorption of hydrolysis products of the parent

Corresponding author: Yue-sheng GAO, E-mail: ygao4@mtu.edu
DOI: 10.1016/S1003-6326(21)65640-6

metal ion [10]. Both mechanisms can explain most of the flotation results. However, their limitation starts to appear when it comes to unconventional flotation phenomena, urging for new explanations. Under this circumstance, more and more theoretical and practical mechanisms have been suggested to solve the predicament. For instance, from the liquid film stability point of view, metal ions in the slurries might affect the drainage of liquid film between minerals and bubbles prior to the attachment [11].

In previous work, a systematic review on this topic was published [12]. However, with the continuous efforts from researchers worldwide, more results and analyses have been reported. Thus, an updated review is in desperate need. Furthermore, powerful research techniques, contributing a lot to the understanding of governing mechanisms, will be presented in this work.

2 Direct and indirect factors

The key factors influencing the roles of metal ions in flotation can be divided into two categories: direct and indirect, as shown in Fig. 1. The direct factors mainly refer to the intrinsic properties of metal ions, such as ion type, radius, valence, and concentration. On the other hand, the indirect factors relate to the ambient environment where metal ions are located, including the operations, pH, reagents, and minerals. Table 1 summarizes metal ions of interest in flotation, as well as their properties. More details are provided in the following paragraphs.

Fig. 1 Factors influencing roles of metal ions in flotation

Table 1 Basic parameters of metal ions commonly involved in flotation

Type	Valence	Radius/Å	Reference
K	+1	1.38	[13]
Cu	+2	0.71	[14]
Ni	+2	0.78	[15]
Pb	+2	1.32	[15]
Mg	+2	0.72	[16]
Ba	+2	1.34	[17]
Mn	+2	0.80	[14]
Ca	+2	1.00	[16]
Co	+2	0.82	[15]
Zn	+2	0.74	[17]
Al	+3	0.535	[18]
Fe	+3	0.64	[19]

2.1 Direct factors

2.1.1 Type of metal ions

Flotation results can vary with the types of involved metal ions. FORNASIERO and RALSTON [20] found that quartz could be well floated when using xanthate as the collector in the presence of either Cu^{2+} or Ni^{2+}. However, in the pH range of 7−10, Cu^{2+} performed more efficiently as an activator ion than Ni^{2+}. FUERSTENAU et al [7] found that quartz could be activated by Pb^{2+} in the pH range of 5.8−8.5, but Mg^{2+} was not an excellent activator under the same conditions. Besides, metal ions in a flotation system may exhibit mutual influences. For example, it is challenging to separate sillimanite and microcline in the presence of Al^{3+}. Because Al^{3+} will serve as an activator and lead to high recoveries of both minerals. However, its activation was significantly weakened in the presence of Fe^{3+} in the slurry [21].

Explanations of the phenomena have been suggested to lie in the interactions between metal ions and mineral surfaces. FENG et al [22] reported both Cu^{2+} and Ca^{2+} could promote the adsorptions of carboxymethyl cellulose (CMC) on chlorite surfaces, but the interactions involved are not the same. Copper ions facilitated CMC adsorptions by being adsorbed onto the mineral surface, and consequently weakening the electrostatic repulsion between the CMC and minerals. In contrast, calcium ions enhanced the CMC adsorption by interacting with the CMC molecules and forming

complexes adsorbed on mineral surfaces.

Besides, different valence states of metal ions engender different flotation results. Generally, monovalent metal ions are less active compared with divalent and trivalent metal ions. Meanwhile, divalent and trivalent cations are not identical in terms of affecting the flotations, either. For instance, Al^{3+} and Fe^{3+} can strongly inhibit the flotation of cyanite, while Ca^{2+} and Mg^{2+} can activate cyanite in the meantime [23].

2.1.2 Radius and valence state of metal ions

The flotation results are closely associated with the radius and valence states of involved metal ions. Indeed, different metal ions have different radii, even if they have the same valences. ZACHARA et al [24] summarized the order of the adsorption capacity of divalent ions on the calcite surfaces: $Cd^{2+}>Zn^{2+}\geq Mn^{2+}>Co^{2+}>Ni^{2+}\gg Ba^{2+}=Sr^{2+}$, which is more or less consistent with the atom radius order. Theoretically, the adsorption capacity of one certain metal ion is closely related to the hydration energy, which is calculated by the following equation:

$$E_{hyd}=E_{metal\ ion\text{-}water}-(E_{metal\ ion}+E_{water}) \quad (1)$$

where $E_{metal\ ion\text{-}water}$ refers to the energy of the metal ion-water cluster; $E_{metal\ ion}$ and E_{water} denote the energy of the metal ion and water system, respectively [25].

Metal ions with high hydration energies exert relatively small adsorption capabilities on calcite surfaces. In contrast, metal ions with low hydration energies tend to form hydroxyl complexes and precipitations on the calcite surface, causing mineral surfaces hydrophobic. Furthermore, it is generally considered that larger atoms possess higher hydration energy, which can be used to illuminate the order mentioned above.

In addition, the ionic radius is an essential factor influencing the ion-exchange in mineral surface lattices. DEMIR et al [26] studied the flotation separation of potassium feldspar and sodium feldspar, elaborating that Ca^{2+} can replace Na^{+} in the crystal lattice of Na-feldspar, while Ba^{2+} can replace K^{+} in the crystal lattice of K-feldspar. The primary reason is that the ionic radii of Na and Ca cations (0.98 and 0.99 Å) and those of K and Ba cations (1.33 and 1.38 Å) are incredibly close. After the replacement of Na^{+} by Ca^{2+} on the Na-feldspar surface, its electronegativity will decrease, rendering a weak flotation recovery.

2.1.3 Concentration of metal ions

Metal ion concentration is another crucial factor. MENG et al [27] studied the activation by lead ions in the ilmenite flotation using benzyl hydroxamic acid (BHA) as the collector. They found that when using 120 mg/L BHA at pH 8.0, the adsorption amount of BHA on ilmenite surfaces increased with increased lead ion concentration. When the Pb^{2+} concentration was higher than 2.0×10^{-4} mol/L, both recovery and BHA adsorption amount increased slowly prior to reaching a plateau.

Metal ions can also cause an inhibitory effect on minerals, especially at high concentrations. It is reported that Mg^{2+}, Ca^{2+} and K^{+} significantly enhance the adsorption of CMC onto talc by changing the adsorption morphology [28]. The increase of Mg^{2+}, Ca^{2+} and K^{+} concentrations caused the coiling of the carbon chain in CMC, leaving more space for further CMC adsorption, and consequently enhancing the CMC coverage on the talc surface.

2.2 Indirect factors

2.2.1 Minerals in slurry

When different minerals exist in the slurry, the roles of metal ions in flotation may be altered, even reversed. For example, in the flotation separation of zircon and cassiterite using NaOL as the collector, Fe^{3+} can depress the cassiterite flotation while it can activate the zircon flotation at the same time [6].

The underlying mechanism might lie in the mineral crystal structure, which is recently attracting intense attention. Different crystal faces of the same mineral will result in difference in polarity, electrical properties, and solubility, which is known as anisotropy [29−32]. For instance, the activation of sphalerite (ZnS) flotation is commonly seen using Cu^{2+} [33,34]. Still, the activation of smithsonite, another Zn-containing mineral, by Cu^{2+} has yet been reported, which is related to the bond types and coordination numbers of Zn in crystal structures of mineral surfaces. Additionally, element substitutions can cause structural changes in minerals and then flotation behaviors. For example, BOULTON et al [35] found that iron ions substituted in the mineral lattice could weaken the activation of sphalerite. Besides, the presence of other minerals may affect the impact of metal ions on flotation. FINCH et al [36] investigated the

pyrite floatability using Cu^{2+}, Fe^{3+}, and Ca^{2+} ions as activators, and they concluded that these metal ions could activate pyrite flotation. However, the system is required to be free of sphalerite.

2.2.2 Solution pH

The pH of the slurry represents the relative content of H^+ and OH^- in the solution, which can affect the existing forms of metal ions and the surface electrical properties of minerals. To achieve the best out of metal ions in flotations, there are specific optimal pH ranges, as summarized in Table 2.

Table 2 Preferred pH range for mineral flotation in the presence of metal ions

Mineral	Collector	Metal ion	Preferred pH range	Reference
Quartz	Sodium oleate	Fe^{3+}	5−6	[37]
		AL^{3+}	3.8−8.4	
		Pb^{2+}	6.5−12	
		Mn^{2+}	8.5−9.4	[38−41]
		Mg^{2+}	10.9−11.7	
		Ca^{2+}	>12	
	Xanthate	Ni^{2+}	7−10	[20]
		Cu^{2+}	7−10	
		Pb^{2+}	6−12	[42]
Cassiterite	Benzohydroxamic acid	Fe^{3+}	8	[43,44]
		Pb^{2+}	7−8	[45,46]
Sphalerite	Potassium ethyl xanthate	Pb^{2+}	9	[47−49]
Smithsonite	DDA	Fe^{3+}	11	[50]
Galena	Xanthate	Ca^{2+}	9.5	[4]
Pentlandite	SBX	Al^{3+}	8.5	[51]

Generally, pH can affect the impact of metal ions on flotation in two ways. For one thing, the metal ion species in solution varies at different pH values. Under the optimal pH range, the active metal ion species will distribute in their appropriate forms. Take the activation of sphalerite by Pb^{2+} as an example, the activating entity is lead ion on mildly acidic conditions while that changes to lead hydroxide on mildly alkaline conditions. RASHCHI et al [52] found that lead activation on sphalerite flotation is dependent on pH values. Specifically, Pb^{2+} is the dominant species when pH≤7, where sphalerite can be effectively activated. While at pH 10 and 11, the dominant species shifts to $Pb(OH)_{2,s}$, where the activation ceases.

It is suggested that activation reactions can vary with pH values. Table 3 shows the comparison of activation steps in sphalerite flotation at different pH values. The activation is remarkable in acidic media, as metal ions tend to be fixed on sphalerites surface by lattice substitution with Zn^{2+}. While in a weak alkaline medium, metal ions adsorb on sphalerite surfaces in the form of sulfide precipitate, which is easily redissolved into the solution. Therefore, the optimum pH for metal ion activation of sphalerite is not in the weak alkaline range.

Table 3 Comparison of activation steps of sphalerite flotation by metal ion at different pH

pH	Reaction	Reference
Weak acid medium	$M^{2+}_{aq} \rightarrow M^{2+}_{aq,s}$ $M^{2+}_{aq,s} \rightarrow M^{2+}_{ads}$ $M^{2+}_{ads} \rightarrow M^{2+}_{lattice}$ $Zn^{2+}_{lattice} \rightarrow Zn^{2+}_{ads}$ $Zn^{2+}_{ads} \rightarrow Zn^{2+}_{aq,s}$ $Zn^{2+}_{aq,s} \rightarrow Zn^{2+}_{aq}$	[53]
Neutral or weak alkaline medium	$M^{2+}_{aq} + 2OH^- \Leftrightarrow M(OH)_{2_s}$ $M(OH)_{2_s} + ZnS_s \Leftrightarrow$ $(Zn,M)S_s + Zn^{2+}_{aq} + 2OH^-$ $M(OH)_{2_s} \Leftrightarrow M^{2+}_{aq} + 2OH^-$ $Zn^{2+}_{aq} + 2OH^- \Leftrightarrow Zn(OH)_{2_s}$	[54]

M−Cu, Pb, Cd, etc.; aq−In solution; s−On mineral surface; ads−At surface active site; lattice−In lattice

2.2.3 Flotation agents

The joint agents, mainly including collectors, regulators, depressants, or inhibitors in flotation, also affect the roles of metal ions. Because of the interactions between agents and metal ions, metal ions can promote the adsorption of anionic collectors on the mineral surfaces but weaken the interaction between cationic collectors and minerals [37]. Apart from these, metal ions alter the interaction between inhibitors and minerals. Dextrin, a standard inhibitor, was barely adsorbed on pyrite surfaces. However, in the presence of Fe^{2+} and Pb^{2+}, its adsorption amount reached 0.45 and 0.3 mg/g, respectively, indicating that some metal ions could promote the adsorption of dextrin, probably via the formation of metal ion-dextrin complexes [55].

The collectors can also modify the distribution of metal ion species in slurries. Spectral analysis

shows that flotation agents can form chelates with metal ions [56]. For instance, BHA can chelate with Pb^{2+} to form a five-membered ring structure, which in turn reduces the concentration of metal ions in the slurry [57,58]. Besides, in the pyrite flotation system, the total iron concentration detected in the slurry was doubled with the addition of xanthate [59], indicating the collector might facilitate the extraction of metal ions from the minerals.

2.2.4 Operations

Operations like the adding sequence of metal ions and flotation reagents have been recently found to have a significant impact on flotation. Typically, the metal ions are added into the flotation system prior to the addition of reagents. However, when premixing metal ions and reagents to form complexes, a more vital collecting ability couple with a higher selectivity have been frequently reported in the past few years.

TIAN et al [56,57] found a soluble lead-BHA complex, obtained by premixing lead nitrate and BHA in a separated container, performed much better in the cassiterite flotation, compared with the traditional sequential addition of lead nitrate (LN) and BHA. HAN et al [60] observed the adsorption amount and intensity of BHA on scheelite surfaces were more considerable when adding the lead-BHA complex. Other researchers followed similar tracks and confirmed conclusions by launching the flotation of scheelite, ilmenite, and titanaugite [44,61,62].

3 Underlying mechanisms

3.1 Oxide and silicate minerals

Oxide and silicate minerals are widely distributed in the Earth's crust. When it comes to revealing the interactions between metal ions and minerals, they can be discussed using the same electrostatic model [63,64]. In this area, two classic mechanisms of interactions between metal ions and minerals have been well-appreciated.

The first traditional mechanism comprises two steps. Its schematic is provided in Fig. 2. Firstly, metal ions react with OH^- on mineral surfaces, releasing water molecules and forming hydroxide species, namely active sites. Subsequently, collectors adsorb the active sites to render the surface hydrophobic.

FUERSTENAU and RAGHAVAN [9] suggested that metal ions could react with OH^- in the pulp and adsorb on minerals surface as a metal cation complex, forming an active site that can interact with the flotation agents, consequently adjusting the hydrophobicity of the mineral surface.

However, some researchers [65] hold a different view and proposed an alternative mechanism: the adsorption of metal ions on mineral surfaces and the subsequent activation of flotation cannot be solely attributed to the formation of a hydroxy complex. Instead, the formation of metal hydroxide surface precipitation should be a more effective way, as shown in Fig. 3.

JAMES and HEALY [66] reported that the solubility of the metal hydroxide produced at the mineral−water interface is smaller than that in water due to a more modest change of Gibbs free energy. Therefore, metal hydroxides are easily formed at the mineral−water interface. A summary of commonly-seen metal hydroxides is given in Table 4.

Both mechanisms can explain the roles of metal ions in most of the flotation processes; nevertheless, with observations of some exceptional

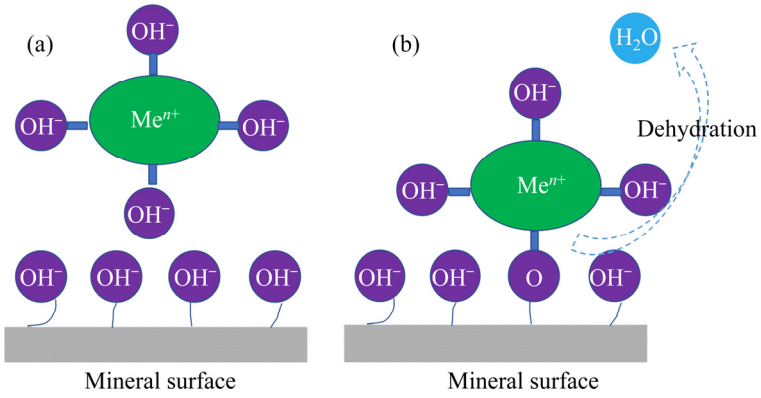

Fig. 2 Formation of metal ion-hydroxy complex on mineral surface: (a) Before interaction; (b) After interaction

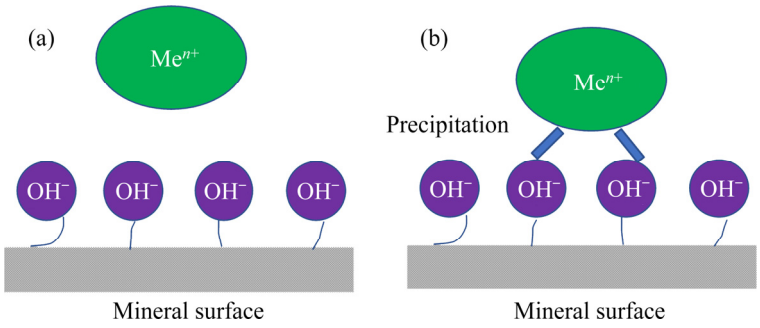

Fig. 3 Formation of metal hydroxide precipitation on mineral surface: (a) Before interaction; (b) After interaction

Table 4 Active components of different metal ions in flotation system of oxide and silicate minerals

Mineral	Metal ion	Active species	Reference
Quartz	Pb^{2+}	$Pb(OH)^+$, $Pb(OH)_2$	[38,42]
	Mg^{2+}	$Mg(OH)^+$, $Mg(OH)^{2+}$	[40,67]
	Cu^{2+}	$Cu(OH)_2$	[20]
Talc	Ca^{2+}	$Ca(OH)^+$	[68,69]
Spodumene	Ca^{2+}	$Ca(OH)^+$	[70,71]
	Mg^{2+}	$Mg(OH)^+$	
Rutile	Pb^{2+}	$Pb(OH)^+$	[72,73]

phenomena, other means have been proposed. For instance, FUERSTENAU et al [74,75] reported cation sulfonates, functioning as the collector, precipitated immediately in the flotation of beryl and quartz. Recent researches [56,76] demonstrated that a soluble metal-organic complex (lead-BHA complex), produced by premixing lead nitrate and BHA, exhibited an enhanced collecting ability and selectivity in the flotation of cassiterite. A novel activation model was then proposed: metal ions can directly react with the collector and form a cation-collector complex or precipitation, which serves as the "real" collector in the flotation, as illustrated in Fig. 4, where cassiterite is taken as an example. This mechanism is in good agreement with the results in other reports [43,57,77].

3.2 Sulfide minerals

The flotation of sulfide minerals has been a research hotspot for more than a century. It is widely known that most of the sulfide minerals, like pyrite, chalcopyrite, and galena, are readily floated in the presence of thiol collectors [78]. However, sphalerite responds poorly to the short-chain thiol collectors. To enhance its flotation, some metal

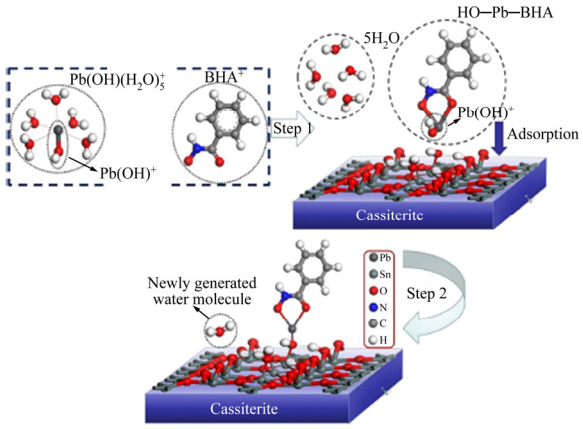

Fig. 4 Formation of metal ion-collector complex as actual collector on mineral surface [57]

ions, such as Cu^{2+}, Pb^{2+}, Cd^{2+}, Fe^{2+}, are applied to activating sphalerite. Simultaneously, some sulfide minerals can be inadvertently activated by metal ions, which might be detrimental to the selective separation of sphalerite from other sulfide minerals, especially pyrite. The activation often occurs in either acidic or alkaline circuits, seldomly at a neutral pH. The formation of ternary surface complexes (M-OH-X) at the mineral surface is probably the main reason for the inhibition at neutral pH [79−81]. Other researchers reported similar results. LASKOWSKI et al [82] attributed the low recovery at nearly neutral pH to the formation of $CuOH^+$. The activation mechanism generally consists of two processes, i.e., ion-exchange reaction and electrochemical reaction, based on some comprehensive reviews [83−86]. In acidic pH pulp, the ion-exchange reaction can be expressed as

$$MeS+M^{2+}\rightarrow MS+Me^{2+} \quad (2)$$

where MeS is the sulfide on the mineral surface to be activated, and MS is the product of the ion exchange. It has been well documented

that the exchange ratio, defined as $R=[M^{2+}]_{exchanged}/[Me^{2+}]_{exchanged}$ [53,54], is close to unity [34,85−87]. The activation of sphalerite in flotation has been well investigated and will be taken as an example in this section. It is generally agreed that the ion-exchange reaction between Cu^{2+} and sphalerite can be written as

$$ZnS_{(surf)}+Cu^{2+}_{(aq)}\rightarrow CuS_{(surf)}+Zn^{2+}_{(aq)} \quad (3)$$

which is thermodynamically favorable [82]. However, it is a different scenario for the alkaline pulp, where precipitation would appear in the form of the activator-metal hydroxide on sphalerite surfaces. Then, precipitation would be converted to the thermodynamically stable substance through an ion-exchange reaction [83,85], as

$$ZnS_s+Cu^{2+}_{(aq)}+2H_2O\rightarrow ZnS_sCu(OH)_{2surf}+2H^+ \quad (4)$$

$$Cu(OH)_{2,ads}+ZnS_{surf}\rightarrow CuS_{surf}+Zn(OH)_{2,ads} \quad (5)$$

or,

$$yZnS+xCu^{2+}+2x(OH^-)\rightleftharpoons yZnS+xCu(OH)_2\rightleftharpoons yZnS\cdot xCu(OH)_2 \quad (6)$$

$$yZnS\cdot xCu(OH)_2\rightleftharpoons(y-x)(ZnS)xCu^{2+}S^{2+}xZn(OH)_2 \quad (7)$$

Apart from ion-exchange, electrochemical reactions are also taking effect. For example, divalent Cu^{2+} ions adsorbed on the sphalerite surface tend to be reduced to monovalent Cu^+. It has been continuously debated what the final copper activation products are. Here we provide a comprehensive summary for the readers' information, as shown in Table 5.

Table 5 Products of copper activation on sphalerite surface

Main activation products	pH	Steric configuration of Cu	Reference
CuS-like species	9.2	–	[86,88]
Covellite-like species	10−12	Tetrahedrally coordinated form	[89]
$Cu^{0.9+}S_2^{1.63-}$	5.5 or 8.5	Distorted trigonal planar geometry	[87]
Cu(I) species	2 or 5	4-fold coordination	[90]

These activation products then create the complex of Cu-xanthate after interacting with xanthate, leaving sphalerite surfaces hydrophobic. However, some researchers believe that $Cu(OH)_2$ directly interacts with xanthate and decomposes to form Cu-xanthate and dixanthogen [34]. More pieces of evidence should be collected to settle the debate with confidence.

4 Research approaches

In this part, various research methods are summarized, which can help to attain a comprehensive and profound understanding of how metal ions take effects in flotation in both macroscopical and microcosmic aspects.

4.1 Micro-flotation tests

Prior to the industrial applications, micro-flotations, or lab-scale flotations, dealing with a feed of 0.002−1 kg, are usually launched to determine a reasonable flowsheet. In this section, key messages are provided considering variables like metal ion dosages, types, valence states, as well as reagents like collectors and depressants.

Micro-flotations show that metal ions can promote the adsorption of inhibitors on the mineral surface, causing a more hydrophilic surface [28,91]. For instance, Ca^{2+} can efficiently enhance the inhibition of talc by CMC in flotation [92]. Figure 5 presents the talc flotation recoveries applying Ca^{2+} concentrations of 0, 1×10^{-4}, 1×10^{-3}, 1×10^{-2} mol/L as a function of CMC dosage at pH 8.5. With the increase of CMC concentration from 0 to 50 mg/L, the flotation recoveries decreased from 93% to 30% when the Ca^{2+} concentration was above 1×10^{-3} mol/L. The results elucidate that CMC has a limited inhibitory effect on talc flotation; however, the depression can be effectively reinforced in the presence of Ca^{2+}.

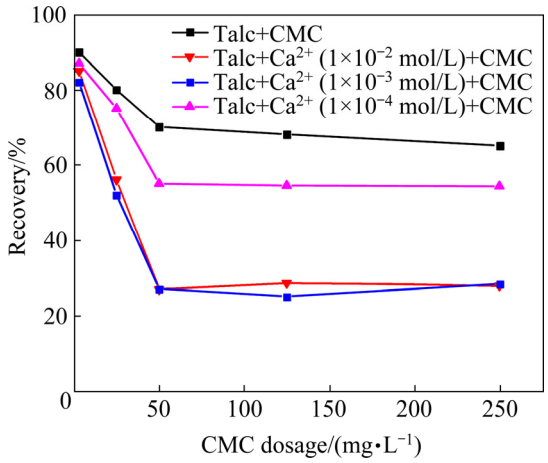

Fig. 5 Recovery of talc in the presence of various Ca^{2+} concentrations as function of CMC dosage at pH 8.5 [92]

On the other hand, the metal ions can facilitate the adsorption of collectors on the mineral surfaces [93−95]. A series of single-mineral flotation experiments were conducted by TIAN et al [43] to investigate the effect of Fe^{3+} on the flotation of cassiterite using BHA as the collector. As shown in Fig. 6, the recovery of cassiterite reached the highest at pH 7, only 30%, in the presence of BHA. In contrast, it increased significantly after adding 10 mg/L ferric chloride, and the highest recovery turned into 80%. It shows that the floatability of cassiterite can be improved by Fe^{3+}.

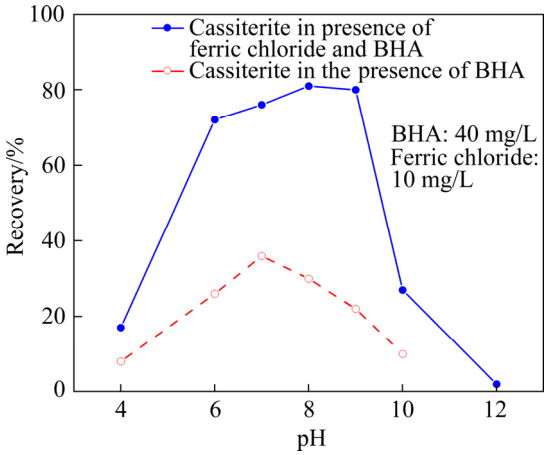

Fig. 6 Flotation recovery of cassiterite as function of pH [43]

4.2 Contact angle measurement

Contact angle measurement is a technique for characterizing solid surface hydrophobicity [96]. To quantify the change of silica surface hydrophobicity, LIU et al [42] measured contact angles of the silica surface on the conditions of different lead ion and potassium amyl xanthate concentrations, and the results are shown in Table 6. It can be seen that a higher contact angle appeared with the increase of lead ion concentration, which means that lead ions may facilitate the xanthate adsorption on the silica surface so that the silica surface becomes more hydrophobicity.

Table 6 Sessile drop contact angles on silica surface for various lead and potassium amyl xanthate concentrations at different pH values (lead concentration equals the amyl xanthate concentration) [42]

Concentration/ (mol·L^{-1})	Contact angle/(°)			
	pH 7.0−7.5	pH 8.0−8.5	pH 9.0−9.6	pH 10.0−10.5
1×10^{-4}	38	27	55	64
5×10^{-4}	80	80	62	74
1×10^{-3}	88	85	81	93

4.3 Zeta potential measurement

The zeta potential measurement is a conventional method to determine the electrokinetic properties on mineral surfaces. Zeta potential is an excellent indicator of the distribution of metal ions near mineral surfaces since it will vary with electrolyte concentrations. For instance, the experimental zeta potential and theoretical surface charge of TiO_2 change with KNO_3 concentrations, as depicted in Fig. 7.

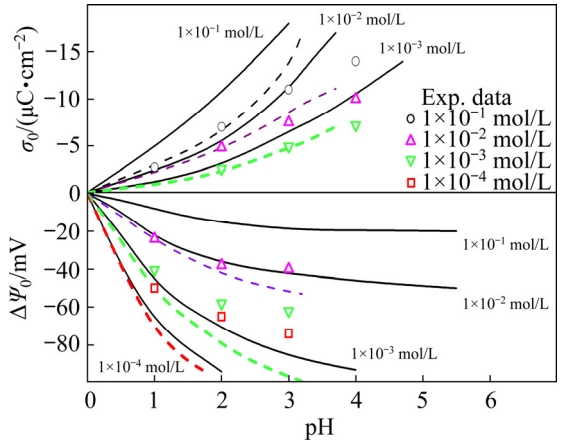

Fig. 7 Comparison of experimental data for zeta potential and surface charge with theoretical predictions of TiO_2 in KNO_3 solutions with different concentrations [97]

To fundamentally understand the relations between metal ions and zeta potentials, one should first understand the establishment of the surface charge. There are two well-known mechanisms.

(1) Hydrogen or hydroxyl ions adsorbing towards mineral surfaces

$$MOH_2^+ \xleftarrow{H^+} MOH \xrightarrow{OH^-} MO^- + H_2O \quad (8)$$

(2) Forming hydroxylated metal species and depositing on mineral surfaces

$$M^{n+} + xOH^- \rightarrow M(OH)_x^{(n-x)+} \quad (9)$$

$$M(OH)_x^{(n-x)+} + OH^- \rightarrow M(OH)_{x+1}^{(n-x-1)+} \quad (10)$$

$$M(OH)_{x+1}^{(n-x-1)+} + H^+ \rightarrow M(OH)_x^{(n-x)+} + H_2O \quad (11)$$

In both mechanisms, concentrations of metal ions, hydrogen, or hydroxyl ions will affect the surface potential's final state, consequently

influencing the flotation. Zeta potentials were usually obtained as a function of pH [98], and their differences before and after adding metal ions or reagents hold the key to interactions, especially the electrostatic interaction.

Explicitly, the interactions between metal ions, reagents, and mineral surfaces can be represented by the shifts of zeta potentials [99−101]. For example, in order to study the influence of Fe^{3+} on the cassiterite flotation, TIAN et al [43] carried out a series of zeta potential measurements, and the results are shown in Fig. 8. In the presence of 10 mg/L ferric chloride, the negative shift of zeta potential of cassiterite sharply increased, indicating that Fe^{3+} can actively enhance the adsorption of BHA on the cassiterite surface. And zeta potential results were also consistent with flotation experiments in Fig. 6 [43] .

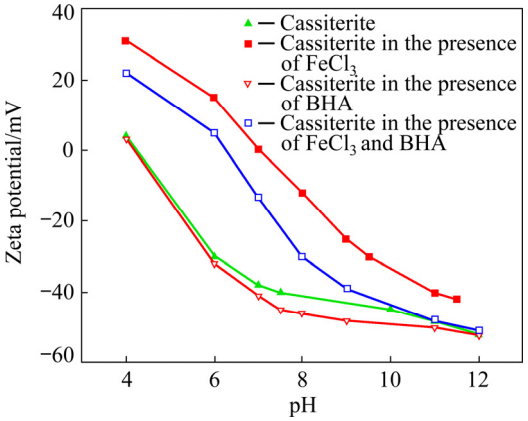

Fig. 8 Zeta potential of cassiterite in the presence and absence of Fe^{3+} as function of pH in the absence and presence of BHA [43]

The zeta potential measurements by FENG et al [102] suggested that the addition of lead ion negatively shifted the zeta potential of cassiterite in the presence of SHA, as shown in Fig. 9. The finding confirms the enhanced adsorption density of SHA on the cassiterite surfaces preoccupied by lead ions.

4.4 Adsorption amount of measurement

Some researchers attempted to quantitively characterize the interaction intensity between collectors and mineral surfaces by launching the adsorption tests [101,103]. The adsorption mechanisms are proposed to be hydrolysis and precipitation on mineral surfaces, referring to the zeta potential section. Some features in the

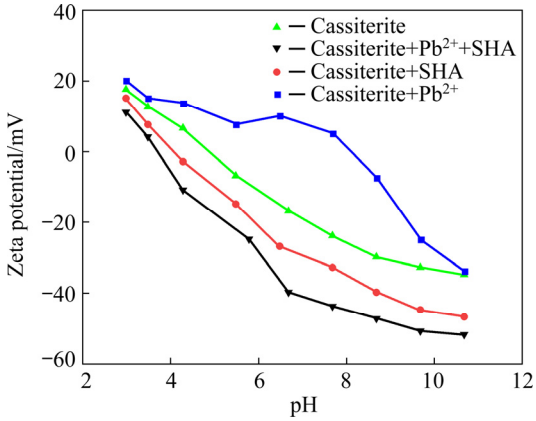

Fig. 9 Zeta potential of cassiterite in the presence and absence of lead ions as function of pH in the absence and presence of SHA [102]

adsorptions are worth being highlighted in this review.

(1) The adsorption rate increases from zero to 100% in a critical pH range, which is usually less than 100%. The reason is due to the change of free energy of adsorption, written as

$$\Delta G^0_{\mathrm{ads}_i} = \Delta G^0_{\mathrm{coul}_i} + \Delta G^0_{\mathrm{solv}_i} + \Delta G^0_{\mathrm{chem}_i} \tag{12}$$

where i notes species type, $\Delta G^0_{\mathrm{ads}}$ is the overall adsorption free energy, $\Delta G^0_{\mathrm{coul}}$ is the free energy of Coulomb's interaction (electrostatic interaction), $\Delta G^0_{\mathrm{solv}}$ is the free energy of solvation, and $\Delta G^0_{\mathrm{chem}}$ is the free energy of the chemical reaction.

The $\Delta G^0_{\mathrm{ads}}$ has to be negative for the adsorption to be spontaneous to occur. It is necessary to calculate the individual item to obtain the $\Delta G^0_{\mathrm{ads}}$.

Take the adsorption of Co^{2+} on the SiO_2 surface as an example:

$$\Delta G^0_{\mathrm{coul}}(\mathrm{Co}^{2+}) = -\left|2e\psi_\delta\right| < 0 \tag{13}$$

$$\Delta G^0_{\mathrm{coul}}(\mathrm{Co(OH)}^{+}) = -\left|2e\psi_\delta\right| < 0 \tag{14}$$

$$\Delta G^0_{\mathrm{chem}}(\mathrm{Co(OH)_2}) = \Delta G^0_{\mathrm{chem}}(\mathrm{Co}^{2+}) = \Delta G^0_{\mathrm{chem}}(\mathrm{Co(OH)}^{+}) < 0 \tag{15}$$

Clearly, both $\Delta G^0_{\mathrm{coul}}$ and $\Delta G^0_{\mathrm{chem}}$ are negative; thus, the sign of $\Delta G^0_{\mathrm{solv}}$ will govern the overall free energy, and $\Delta G^0_{\mathrm{solv}}$ can be expressed as

$$\Delta G^0_{\mathrm{solv}_i} = \left(\frac{z_i^2 e^2 N}{16\pi}\right)\left(\frac{1}{r_i + 2r_{\mathrm{w}}} - \frac{r_i}{2(r_i + 2r_{\mathrm{w}})^2}\right)\cdot \left(\frac{1}{\varepsilon_i} - \frac{1}{\varepsilon_{\mathrm{b}}}\right) + \left(\frac{z_i^2 e^2 N}{32\pi}\right)\left(\frac{1}{r_i + 2r_{\mathrm{w}}}\right)\left(\frac{1}{\varepsilon_{\mathrm{s}}} - \frac{1}{\varepsilon_i}\right) \tag{16}$$

where ψ_δ is obtained by the Gouy−Chapman expression with a surface potential given by the Nernst equation, ε is the permittivity, r is atom radius, z is the valence, and e is the electric charge unit, equal to $1.602176634\times10^{-19}$ C.

Successful adsorptions of metal ions occur at the inner Helmholtz plane (IHP), as shown in Fig. 10. For the highly charged species, the solvation energy needed for the ion to penetrate to IHP is so enormous that the adsorption will not occur. In other words, the adsorption of metal ions will not start until a pH is reached where the lower charged hydroxylated species $M(OH)^{(n-1)+}$ begins to appear.

(2) Species types vary with changing pH, and an example is provided in Fig. 11.

(3) The adsorption is not correlated with ion concentration. In contrast, the amount of adsorption for the surface to be saturated corresponds to an ion layer forming at least one hydration sheath.

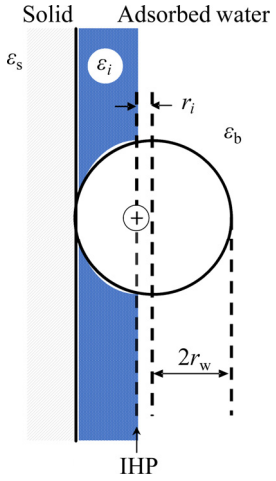

Fig. 10 Schematic of hydrated cation adsorbed at IHP [104]

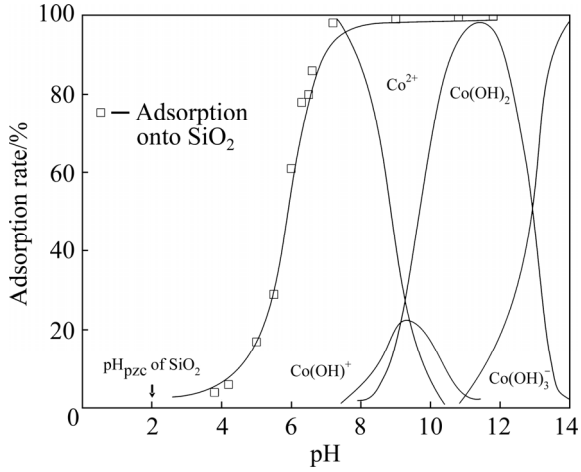

Fig. 11 Experimental adsorption isotherm for Co^{2+} adsorption on silica surface [66]

(4) Adsorption of ions is affected by the surface charges of the mineral; however, the adsorption behavior varies for different minerals even with the same charge. For instance, cobalt ion can adsorb towards TiO_2 even when the surface is slightly positively charged, while it can only adsorb on SiO_2 when its surface is highly negatively charged. On the other hand, the surface charge can be modified and even reversed due to the metal ion adsorption.

(5) The isoelectric point (IEP) of oxide is not influenced by metal ions, indicating that the adsorption type is not chemisorption.

In addition, metal ions are proven to promote the adsorption of collectors on mineral surfaces. TIAN et al [43] found that Fe^{3+} can benefit the adsorption of agents on cassiterite surfaces. As depicted in Fig. 12, the adsorption amount of BHA on the cassiterite surface in the presence of ferric chloride was almost three times as high as that in the absence of ferric chloride, which is in line with the results of flotations and zeta potential measurements in Figs. 6 and 8, respectively.

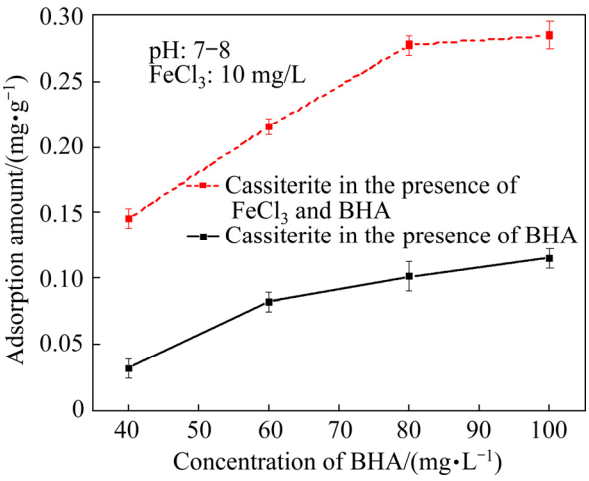

Fig. 12 Adsorption amount of BHA on cassiterite surface as function of BHA concentration in the absence and presence of ferric chloride [43]

Metal ions in the optimum concentration range could facilitate the flotation. SONG et al [105] found that the activation of Ba^{2+} at a low concentration on the flotation of K-feldspar using dodecyl amine chloride as the collector was caused by the ion exchange, which increased the lattice

vacancies and adsorption sites on the mineral surface. Their results are provided in Fig. 13. The recovery of K-feldspar increases from 86.73% to 92.21% as the Ba^{2+} concentration is increased to 1.1×10^{-2} mol/L. After that, the recovery of K-feldspar decreases. The optimum Ba^{2+} concentration to enhance the flotation of K-feldspar is 1.1×10^{-2} mol/L. Once it is above or below this concentration, flotation will be inhibited due to the decreased adsorption sites.

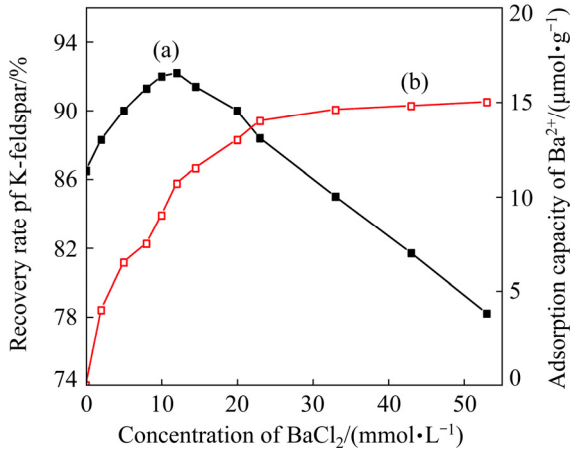

Fig. 13 Recovery rate of K-feldspar versus $BaCl_2$ concentration at 10 mg/L of dodecyl amine chloride addition (a) and effect of $BaCl_2$ concentration on adsorption capacity of Ba^{2+} on surface of K-feldspar (b) [105]

4.5 Imaging analysis techniques

To further extract details of the morphology mineral surfaces in the absence and presence of metal ions, researchers utilize imaging analysis approaches like atomic force microscopy (AFM) and scanning electron microscope (SEM) to visualize the dynamic interaction.

SEM image can display a two-dimensional morphology of the sample surface, via which one can ascertain crucial information, such as the particle size and low dimensional morphology of the mineral surface. YANG et al [106] investigated how the flotation of molybdenite was significantly depressed by Cu^{2+} and Fe^{3+}. They found that Cu and Fe elements evenly and intensively distributed on the molybdenite surface from the EDX mapping in Fig. 14. This is a good piece of evidence proving that a large amount of Cu and Fe species were adsorbed on the molybdenite surface, leading to depression of molybdenite flotation.

Additionally, three-dimensional morphology and flatness of the surface can be obtained by AFM. JIN et al [69,92] revealed that the Ca^{2+} concentration had a significant impact on the morphology of CMC adsorbed on the talc surface. Height and phase are typical messages when analyzing the AFM results: The former represents the straightforward topography of the adsorbed layers, and the latter indicates the hard or soft nature. The AFM images of CMC in the presence and absence of different Ca^{2+} ions concentrations can be seen in Figs. 15−17.

From the images above, when CMC was added alone, the morphology of the talc surface presented the random distribution of salient points, occupying a low coverage. In contrast, salient points were combined, and reticulated adsorption appeared in the presence of 10^{-4} mol/L Ca^{2+}. Moreover, reticulate multilayer adsorption with a high coverage occurred when increasing Ca^{2+} concentration to 10^{-3} and 10^{-2} mol/L Ca^{2+}. The results prove that CMC adsorption on the talc surface can be facilitated when pretreated with Ca^{2+}, consequently enhancing the depression of talc by CMC.

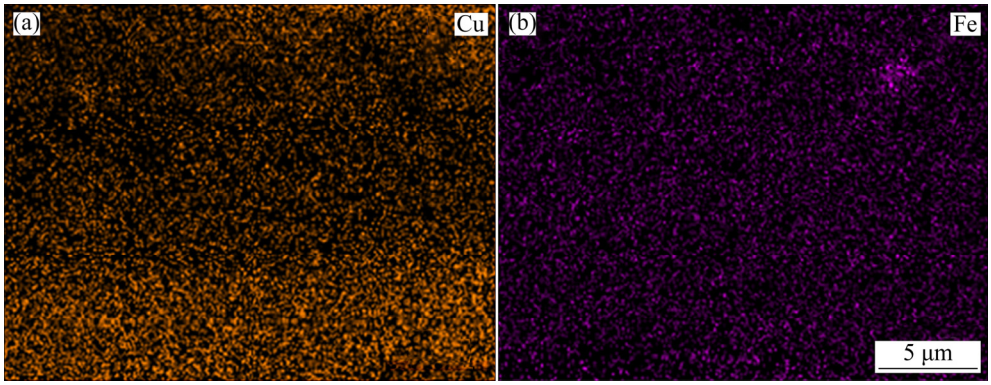

Fig. 14 SEM images of molybdenite sample conditioned in Cu^{2+}(a) and Fe^{3+}(b) solution [106]

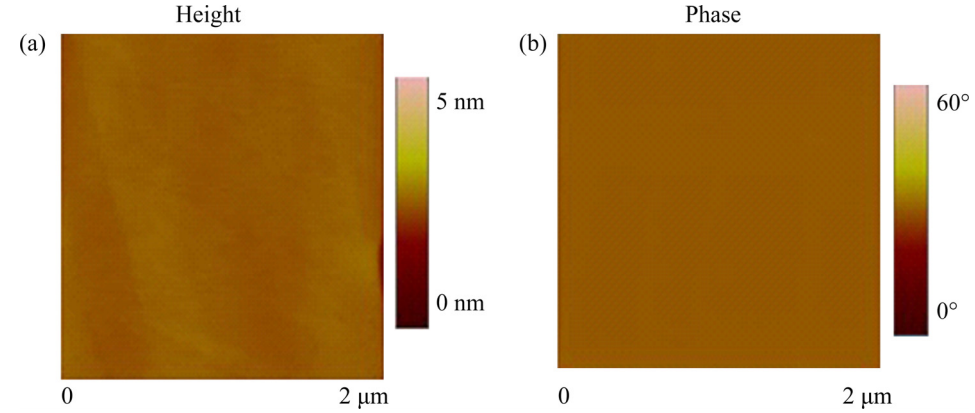

Fig. 15 AFM images of bare talc: (a) Height; (b) Phase [69]

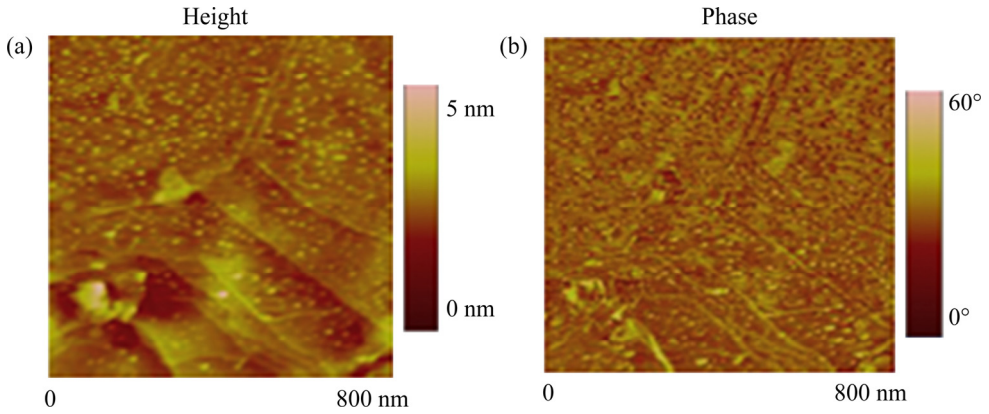

Fig. 16 AFM images of adsorbed CMC (100 mg/L) on talc surface in the absence of ions: (a) Height; (b) Phase [69]

4.6 Surface composition analysis techniques

Surface analysis techniques are also applied to identifying the active metal ion species on mineral surfaces. Fourier transform infrared spectroscopy (FT-IR), and X-ray photoelectron spectroscopy (XPS) are the most widely used methods [107]. Besides, time-of-flight secondary ion mass spectrometry (ToF-SIMS), extended X-ray absorption fine structure (EXAFS), near edge X-ray absorption fine structure (NEXAFS), and the high-resolution AFM have been intensively utilized to visualize the surface components [108].

LIU et al [109] investigated the effects of Ca^{2+} and Mg^{2+} ions on the flotation of spodumene using NaOL as the collector by FT-IR. The results are shown in Figs. 18 and 19.

As shown in the results, new absorption peaks at 1634.75, 2928.49, and 2857.20 cm^{-1} were observed in the spectra of activated spodumene after the addition of Ca^{2+} and Mg^{2+} ions, which manifested the appearance of new species on the mineral surfaces. The peaks were assigned to hydroxy complexes ($CaOH^+$ and $MgOH^+$) and precipitates ($Ca(OH)_2$ and $Mg(OH)_2$).

Mineral surfaces can be elementarily detected by measuring the change in chemical bonds under the FT-IR analysis. But in order to get a better understanding of the reaction mechanism, XPS could be a more powerful tool. CHEN et al [110] detected oxygen and iron on the ilmenite surface and sequentially obtained the status and the relative abundance of the elements. The results are shown in Tables 7 and 8.

In Table 7, a Fe−O−Pb complex was observed at the new peak at about 712.4 eV, which will serve as the activated sites. Similarly, in Table 8, the new peak was obtained at 532.3 eV, which was also contributed to Fe−O−Pb complex. Both results illustrate that the lead ions adsorbed onto the ilmenite surface by reacting with Fe−O−H, imparting active sites for sodium oleate and rendering a surface hydrophobic.

4.7 Computational method

In order to further explore the activation mechanism of metal ions, researchers have built the

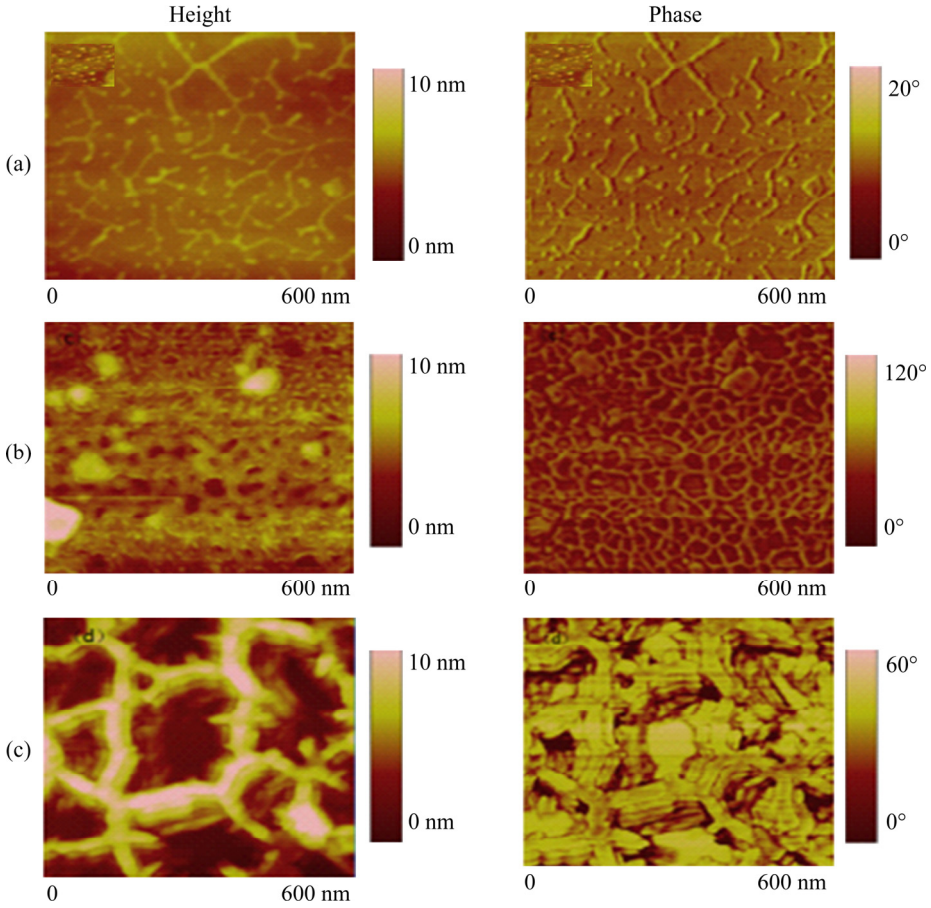

Fig. 17 AFM height and phase images of adsorbed CMC (100 mg/L) on talc surface in the presence of 10^{-4} mol/L (a), 10^{-3} mol/L (b), and 10^{-2}mol/L (c) Ca^{2+}, at pH 8.5 [69]

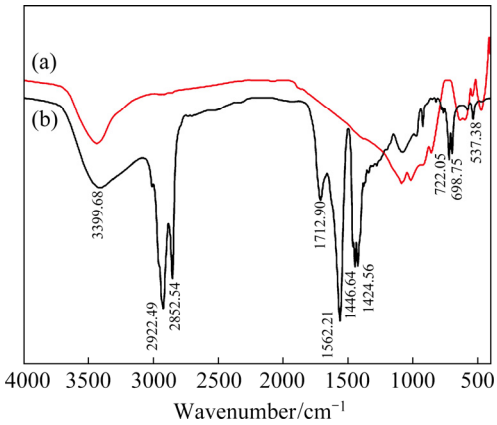

Fig. 18 FT-IR spectra of spodumene (a) and NaOL (b) [109]

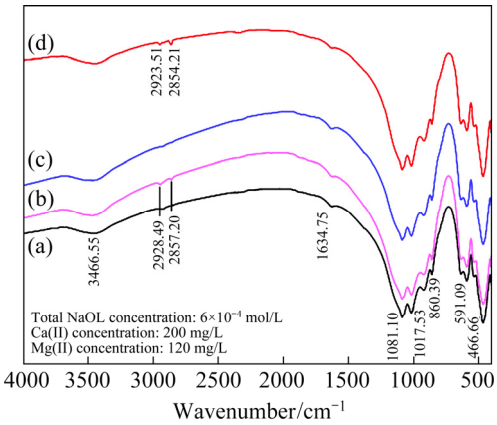

Fig. 19 FT-IR spectra of spodumene with Ca (II) ions at pH 12.5 (a), with Ca (II) ions and NaOL at pH 12.5 (b), with Mg (II) ions at pH 10.0 (c), and with Mg (II) ions and NaOL at pH 10.0 (d) [109]

adsorption models for the interaction of metal ions and agents, calculating adsorption energies by the first principle calculations based on the density functional theory (DFT).

DFT calculations performed by YU et al [111] proved that the precipitation of calcium hydroxide ($Ca(OH)_2$) on the spodumene surface is the dominant active species. They positioned Ca^{2+}, $CaOH^+$ and $Ca(OH)_2$ on the spodumene (110) surface after geometry optimizations and then calculated relevant parameters by Cambridge Serial Total Energy Package (CASTEP). The calculation results can be found in Table 9. It shows that the adsorption energies of Ca^{2+}, $CaOH^+$, and $Ca(OH)_2$

on the spodumene surface are −187.14, −350.81, and −523.31 kJ/mol, respectively, confirming that $Ca(OH)_2$ is the steadiest and the most active species.

Table 7 Parameters of elemental Fe 2p and chemical status on ilmenite surface treated with various conditions [110]

Sample	Peak	Binding energy/eV	Status	Area ratio/%
Ilmenite	P1	710.3	Fe (II)	87.39
	P2	713.0	Fe (III)	12.61
Ilmenite+ lead ions	P1	710.5	Fe (II)	60.31
	P3	711.6	Fe−O−Pb complex	26.57
	P2	713.2	Fe (III)	13.12

Table 8 Parameters of elemental O 1s and chemical status on ilmenite surface treated with various conditions [110]

Sample	Peak	Binding energy/eV	Status	Area ratio/%
Ilmenite	P1	529.9	Ti−O	48.24
	P2	531.4	Fe−O	41.68
	P3	532.7	−OH	10.08
Ilmenite+ lead ions	P1	530.0	Ti−O	41.59
	P2	531.5	Fe−O	39.21
	P4	532.3	Fe−O−Pb	12.57
	P3	532.8	−OH	6.63
Ilmenite+ NaOL	P1	529.8	Ti−O	38.83
	P2	531.3	Fe−O−C/ Pb−O−C/Fe−O	48.82
	P3	532.6	−OH	12.35
Ilmenite+lead ions+NaOL	P1	529.8	Ti−O	31.15
	P2	531.3	Fe−O−C/ Pb−O−C/Fe−O	57.18
	P3	532.6	−OH	11.62

Table 9 Adsorption energy of three adsorbates on spodumene surface and formed Ca−O bond length [111]

Adsorbate	Adsorption energy/(kJ·mol^{-1})	Bond length/nm
Ca^{2+}	−187.14	Ca−O1, 0.2053
		Ca−O2, 0.2337
$CaOH^+$	−350.81	Ca−O1, 0.2209
		Ca−O2, 0.2283
$Ca(OH)_2$	−523.31	Ca−O1, 0.2119
		Ca−O2, 0.2278

Besides, researchers compared interactions between collector and mineral surface in the absence and presence of metal ions. In terms of the simulations of the interactions among sphalerite (110) surface, copper, and ethyl xanthate (EX), LIU et al [112] summarized four types of stable interaction models, as outlined in Fig. 20 and Table 10. The function of Cu^{2+} as a bridge is vividly visualized in the schematics in Fig. 20. More importantly, Fig. 20(d) shows that $Cu(OH)_2$ can adsorb on the ZnS surface prior to serving as the bridge. From Table 10, the interaction energies (ΔE_{int}) of EX and activated sphalerite surfaces are more negative than that of EX and the bare sphalerite surface (−87.63 kJ/mol), indicating that it is easier for EX to adsorb onto the Cu-activated sphalerite surface than the bare surface.

4.8 Solution chemistry calculation

It is well-known that the species distribution of metal ions and flotation reagents in pulp is dissimilar at different pH values and concentrations. Therefore, solution chemical calculation method is needed to describe the chemical species, especially the significant active components of metal ions and reagents in the flotation system. The calculation results are usually presented as species distribution diagrams.

TIAN et al [57] found that a high flotation recovery could be obtained when using lead-BHA complex as collector at pH 8−9, and the species diagrams of lead ions and BHA were depicted in Fig. 21. Pb^{2+} ions usually interact with surrounding water molecules to form hydrated lead ions. At pH 6−8, $Pb(H_2O)_6^{2+}$ is the dominant species in the lead nitrate solution. While $Pb(OH)(H_2O)_5^+$ becomes the dominant species at pH 8−10. As for BHA, molecular BHA and BHA^- are the predominant forms at pH 6−8 and 8−9, respectively. Based on the chemistry calculations, the primary active components of the lead-BHA complex at pH 8−9 could be HO−Pb−BHA.

4.9 Cyclic voltammetry

Due to the electrical semi-conductivity, redox reactions frequently occur on the surfaces of many sulfide minerals in an oxygenated environment. In some cases, the sulfide minerals are poorly collected by short-chain thiol collectors without the treatment of activation by metal ions. The cyclic

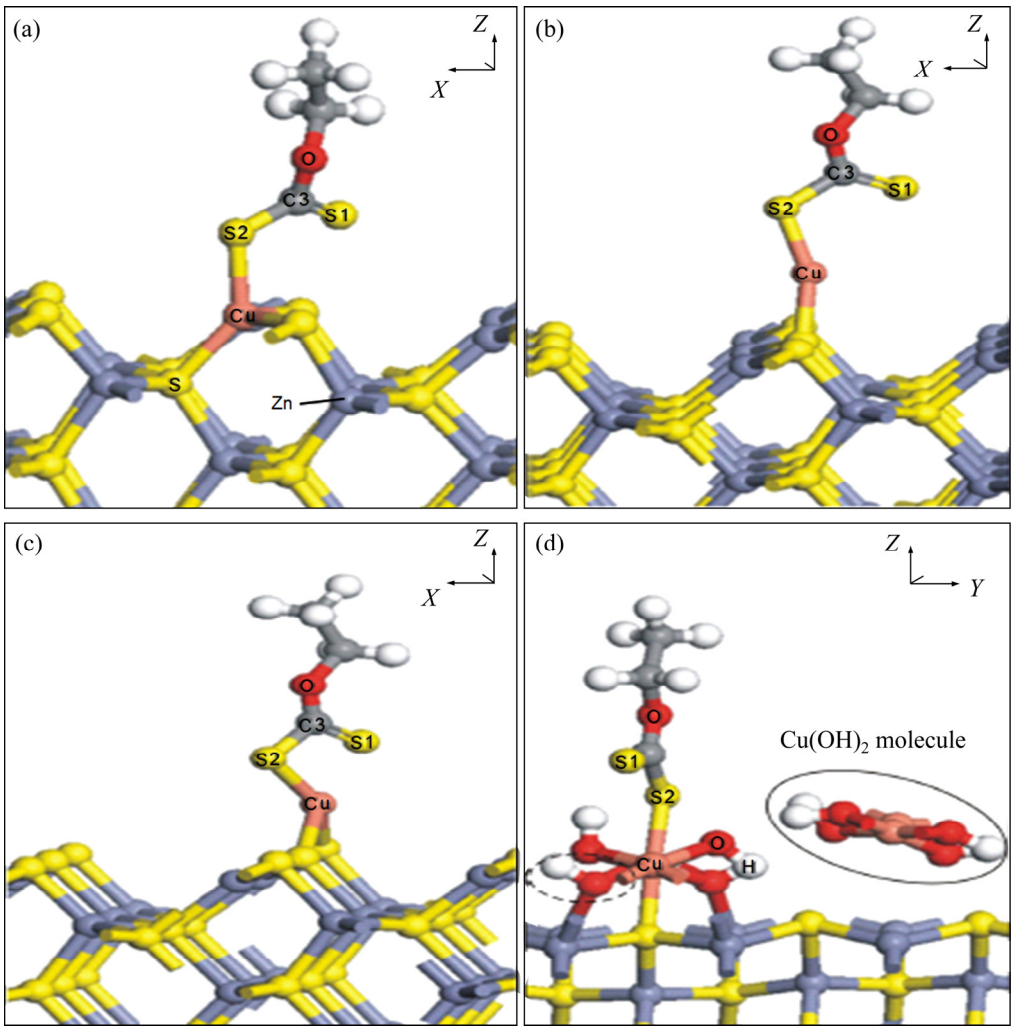

Fig. 20 Schematic of EX interaction with Cu-activated ZnS (110) surface: (a) Substituted Cu; (b) Cu adsorbed on top site of S; (c) Cu adsorbed on bridge site of S; (d) $Cu(OH)_2$ adsorbed on ZnS surface [112]

Table 10 Interaction energy and bond length of Cu—S for four interaction models [112]

Interaction model	ΔE_{int}/(kJ·mol^{-1})	D_{Cu-S}/Å
ZnS (110)−substituted Cu−EX	−232.52	2.24
ZnS (110)−Cu adsorbed on top site of S−EX	−256.11	2.14
ZnS (110)−Cu adsorbed on bridge site of S−EX	−268.65	2.28
ZnS (110)−surface $Cu(OH)_2$−EX	−281.60	2.31

voltammetry, an electrochemical method for quantitative analysis of the parameters like voltage and current during electrolysis, is introduced to reveal the electrical characteristics during the redox reactions involving metal ions.

The activation products by metal ions can be deduced from the anodic and cathodic waves. CHEN and YOON [113] found that a CuS-like activation product was formed on the surface of sphalerite activated by 1×10^{-4} mol/L $CuSO_4$, as shown in Fig. 22.

The anodic wave (A_1) shown in Fig. 22(a) represents the oxidation of the activation products. And the cathodic wave (C_2) shown in Fig. 22(b) represents the reduction of the activation product. The detailed reactions are shown in Table 11. Activation reactions of metal ions on sulfide surface can be quantitatively revealed: compared to a thermodynamic potential of 0.303 V for CuS to be oxidized to S^0, it is simultaneously oxidized to CuS_n as the intermediate step. This cyclic voltammetry provides a straightforward way to understand the activation mechanism of metal ions in sulfide flotations.

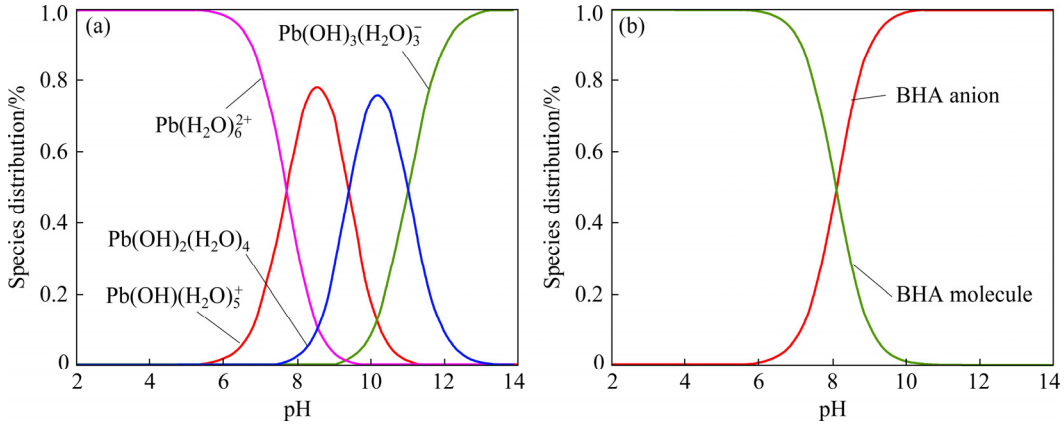

Fig. 21 Species distribution diagrams of lead (a) and BHA (b) in aqueous solution [57]

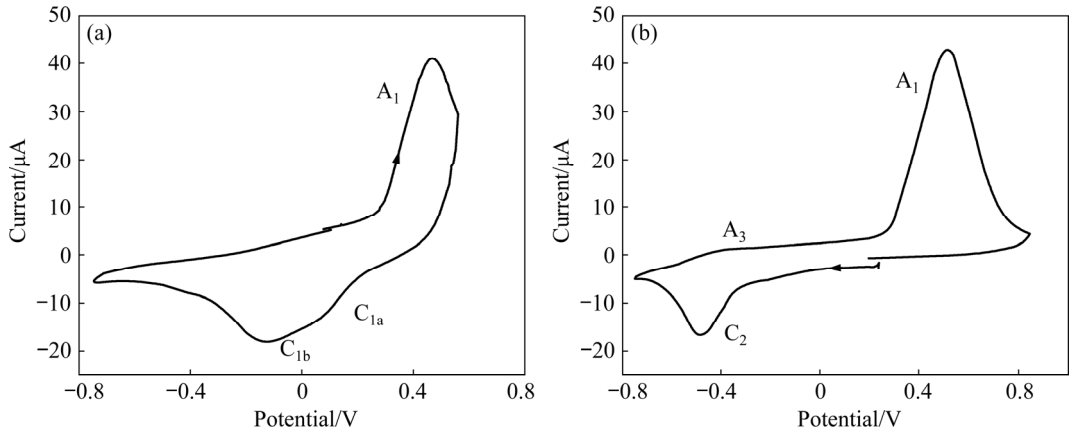

Fig. 22 Voltammograms of CMC: (a) First sweep positive-going scan; (b) First sweep negative-going scan (ZnS electrodes activated for 10 min in deoxygenated 1×10^{-4} mol/L $CuSO_4$ solution at pH 9.2, 0.025 mol/L borate, and sweep rate of 25 mV/s) [113]

Table 11 Activation reactions occurring under anodic and cathodic wave [113]

Peak of wave	Reaction	Thermodynamic potential, E_h/V
Anodic wave	$CuS+H_2O\rightarrow CuO+2H^++S^0+2e$	0.303
	$nCuS+(n-1)H_2O\rightarrow Cu_nS+(n-1)CuO+2(n-1)H^++2(n-1)e$	Below thermodynamic potential for CuS oxidation
Cathodic wave	$2CuS+H^++2e\rightarrow Cu_2S+HS^-$	−0.273

5 Conclusions and future directions

For the mining industry, understanding and utilizing the roles of metal ions in flotation are of both fundamental and practical importance. Thanks to substantial progress that has been accomplished, we are able to comprehensively address this topic here.

The main factors affecting the roles of metal ions in flotations fall into two categories: direct and indirect. Direct factors include metal ion type and valence, radius and valence state, concentration. On the other hand, minerals in the slurry, solution pH, flotation agents, and operations of adding metal ions are placed in the category of indirect factors.

Mechanisms of interactions between metal ions and minerals vary with mineral types. For silicate and oxide minerals, the first possible mechanism contains two steps: the cation and its hydroxide species react with hydroxy on the mineral surface to form activated sites initially; subsequently, the collectors adsorb the active sites to render the surface hydrophobic. An updated assumptive mechanism was proposed in recent years: Metal ions can react directly with the collector and form a cation-collector complex or precipitation, which functions as the real collector in the flotation. As for sulfide minerals,

ion-exchange and oxidation-reduction govern the interactions between metal ions and minerals.

Research approaches like micro-flotation tests, contact angle measurement, zeta potential measurement, adsorption measurement, AFM, SEM, FT-IR, XPS, DFT, calculation of chemical solution, and cyclic voltammetry have been used to investigate the roles of metal ions from both macroscopic and microcosmic perspectives. And findings from one method are in good agreement with others.

However, there is still a lack of technical means to detect specific active sites and forces on mineral surfaces in actual flotation, which is prerequired to quantify interactions between metal ions and minerals as well as flotation agents. Besides, in order to better capitalize the roles of metal ions in flotation and benefit the mining industry, further explorations, notably the real-time detection of metal ions, are in urgent need. Furthermore, endeavors in building simulation models with high accuracies are required to conveniently reconstruct the relevant reaction processes.

Acknowledgments

The authors acknowledge financial supports from the National Natural Science Foundation of China (Nos. U2067201, 51774328), the Key Program for International S & T Cooperation Projects of China (No. 2021YFE0106800), the Science Fund for Distinguished Young Scholars of Hunan Province, China (No. 2020JJ2044), the Young Elite Scientists Sponsorship Program by Hunan province of China (No. 2018RS3011), and the National 111 Project of China (No. B14034). The authors also wish to thank Dr. JOHN RALSTON for the early guidance on this manuscript. And the authors also much appreciate the help from Mr. HASSAN RAZA for improving the language.

References

[1] LI Cheng-wei, GAO Zhi-yong. Effect of grinding media on the surface property and flotation behavior of scheelite particles [J]. Powder Technology, 2017, 322: 386−392.

[2] LI Cheng-wei, GAO Zhi-yong. Tune surface physico-chemical property of fluorite particles by regulating the exposure degree of crystal surfaces [J]. Minerals Engineering, 2018,128: 123−132.

[3] FLORES-ÁLVAREZ J M, ELIZONDO-ÁLVAREZ M A, GUERRERO-FLORES A D, URIBE-SALAS A. Electrochemical behavior of galena in the presence of calcium and sulfate ions [J]. Minerals Engineering, 2017, 111: 158−166.

[4] BULUT G, YENIAL Ü. Effects of major ions in recycled water on sulfide minerals flotation [J]. Minerals & Metallurgical Processing, 2016, 33: 137−143.

[5] ELIZONDO-ALVAREZ M A, FLORES-ALVAREZ J M, DAVILA-PULIDO G I, URIBE-SALAS A. Interaction mechanism between galena and calcium and sulfate ions [J]. Minerals Engineering, 2017, 111: 116−123.

[6] PENG Hui-qing, LUO Wen, WU Di, BIE Xue-xiang, SHAO Hui, JIAO Wen-ya, LIU Yi-ke. Study on the effect of Fe^{3+} on zircon flotation separation from cassiterite using sodium oleate as collector [J]. Minerals, 2017, 7: 1−18.

[7] FUERSTENAU M C, MILLER J D, PRAY R E. Metal ion activation in xanthate flotation of quartz [J]. Society of Mining Engineers, 1965, 232: 359−365.

[8] HU Y, LIU X, XU Z. Role of crystal structure in flotation separation of diaspore from kaolinite, pyrophyllite and illite [J]. Minerals Engineering, 2003, 16: 219−227.

[9] FUERSTENAU D, RAGHAVAN S. Flotation [M]. New York: AIME, 1976.

[10] JAMES R O, HEALY T W. Adsorption of hydrolyzable metal ions at the oxide-water I: Co(ll) Adsorption on SiO_2 and TiO_2 as model systems interface [J]. Journal of Colloid & Interface Science, 1971, 40: 42−52.

[11] GAO Yue-sheng, PAN Lei. Measurement of instability of thin liquid films by synchronized tri-wavelength reflection interferometry microscope [J]. Langmuir, 2018, 34: 14215−14225.

[12] GAO Yue-sheng, GAO Zhi-yong, SUN wei. Research progress of influence of metal ions on mineral flotation behavior and underlying mechanism [J]. Transactions of Nonferrous Metals Society of China, 2017, 27: 859−868.

[13] LIU Yang, RU Qiang, GAO Yu-qing, AN Qin-you, CHEN Fu-ming, SHI Zheng-lu, ZHENG Min-hui, PAN Zi-kang. Constructing volcanic-like mesoporous hard carbon with fast electrochemical kinetics for potassium-ion batteries and hybrid capacitors [J]. Applied Surface Science, 2020, 525: 146563.

[14] SUSETE T B, EÂDER T G, GILBERTO O C. Correlation between ionic radius and thermal decomposition of Fe(II), Co(II), Ni(II), Cu(II) and Zn(II) diethanoldithiocarbamates [J]. Thermochimica Acta, 2000, 356: 79−84.

[15] MEKATEL H, AMOKRANE S, BENTURKI A, NIBOU D. Treatment of polluted aqueous solutions by Ni^{2+}, Pb^{2+}, Zn^{2+}, Cr^{6+}, Cd^{2+} and Co^{2+} ions by ion exchange process using faujasite zeolite [J]. Procedia Engineering, 2012, 33: 52−57.

[16] FENG Qing-rong, GUO Jian-dong, XU Xiao-lio, ZHANG Nan, ZHU Xing, FENG Sun-qi. The effect of ionic radius of metal element (M) on (Pb,M)-1212 superconductors (M=Sr, Ca, Mg, Hg, Cd, Cu) [J]. Solid State Communications, 1995, 94: 21−25.

[17] PINALLI R, DALCANALE E, MISZTAL K, LUCENTINI R, UGOZZOLI F, MASSERA C. Metal ion complexation by tetraphosphonate cavitands: The influence of the ionic radius [J]. Inorganica Chimica Acta, 2018, 470: 250−253.

[18] SHI Lei, HAN Ya-jie, WANG Shuang, MA Di, MAO Zhi-yong, WANG Da-jian, LI Xi-ze, ZHANG Lu, ZHANG Zhi-wei, LU Xu-lin. $NaLa_2SbO_6:Mn^{4+}$ far-red phosphor: Synthesis, luminescence properties and emission enhancement by Al^{3+} ions [J]. Journal of Luminescence, 2020, 219: 116865.

[19] ABOUL M, ABDEL A S, HADDAD A, OMAIMA A. Kinetics and mechanism of ion exchange of Fe^{3+}, Cd^{2+} and Na^+/H^+ on Lewatite S-100 cation exchanger in aqueous and aqueous-detergent media [J]. Journal of Saudi Chemical Society, 2012, 16: 395−404.

[20] FORNASIERO D, RALSTON J. Cu(II) and Ni(II) activation in the flotation of quartz, lizardite and chlorite [J]. International Journal of Mineral Processing, 2005, 76: 75−81.

[21] ZHANG Qi, FANG He-ping. Study on the effect of metallic ions on the flotation separation of sillimanite and microcline [J]. Conservation and Utilization of Mineral Resources, 1999, 1: 32−35.

[22] FENG Qi-ming, FENG Bo, LU Yi-ping. Influence of copper ions and calcium ions on adsorption of CMC on chlorite [J]. Transactions of Nonferrous Metals Society of China, 2013, 23: 237−242.

[23] ZHANG Jin-xia, FENG Ya-li, NIU Fu-sheng. Influence of metal ions in pulp on floatability of kyanite minerals [J]. Journal of Northeastern University (Natural Science), 2014, 35: 1788−1791.

[24] ZACHARA J M, COWAN C E, RESCH C T. Sorption of divalent metals on calcite [J]. Geochimica et Cosmochimica Acta, 1991, 55: 1549−1562.

[25] BODA A, ALI S M. From microhydration to bulk hydration of Rb^+ metal ion: DFT, MP2 and AIMD simulation study [J]. Journal of Molecular Liquids, 2013, 179: 34−45.

[26] DEMIR C, BENTLI I, GULGONUL I, CELIK M S. Effects of bivalent salts on the flotation separation of Na-feldspar from K-feldspar [J]. Minerals Engineering, 2003, 16: 551−554.

[27] MENG Qing-you, YUAN Zhi-tao, LI Yu, XU Yuan-kai, DU Yu-sheng. Study on the activation mechanism of lead ions in the flotation of ilmenite using benzyl hydroxamic acid as collector [J]. Journal of Industrial and Engineering Chemistry, 2018, 62: 209−216.

[28] KHRAISHEH M, HOLLAND C, CREANY C, HARRIS P, PAROLIS L. Effect of molecular weight and concentration on the adsorption of CMC onto talc at different ionic strengths [J]. International Journal of Mineral Processing, 2005, 75: 197−206.

[29] GAO Zhi-yong, LI Cheng-wei, SUN Wei, HU Yue-hua. Anisotropic surface properties of calcite: A consideration of surface broken bonds [J]. Colloids and Surfaces A: Physicochemical and Engineering Aspects, 2017, 520: 53−61.

[30] GAO Zhi-yong, FAN Rui-ying, RALSTON J, SUN Wei, HU Yue-hua. Surface broken bonds: An efficient way to assess the surface behaviour of fluorite [J]. Minerals Engineering, 2019, 130: 15−23.

[31] GAO Zhi-yong, XIE Lei, CUI Xin, HU Yue-hua, SUN Wei, ZENG Hong-bo. Probing anisotropic surface properties and surface forces of fluorite crystals [J]. Langmuir, 2018, 34: 2511−2521.

[32] GAO Zhi-yong, HU Yue-hua, SUN Wei, DRELICH J W. Surface-charge anisotropy of scheelite crystals [J]. Langmuir, 2016, 32: 6282−6288.

[33] PATTRICK R A, ENGLAND K E, CHARNOCK J M, MOSSELMANS J F. Copper activation of sphalerite and its reaction with xanthate in relation to flotation an X-ray absorption spectroscopy [J]. International Journal of Mineral Processing, 1999, 55: 247−265.

[34] POPOV S R, VUCINIC D R. The ethylxanthate adsorption on copper-activated sphalerite under flotation-related conditions in alkaline media [J]. International Journal of Mineral Processing, 1990, 30: 229−244.

[35] BOULTON A, FORNASIERO D, RALSTON J. Effect of iron content in sphalerite on flotation [J]. Minerals Engineering, 2005, 18: 1120−1122.

[36] FINCH J A, BOZKURT V, ZHANG Q, XU Z. Pyrite flotation in the presence of metal ions and sphalerite [J]. International Journal of Mineral Processing, 1997, 52: 187−201.

[37] ZHANG Jie, WANG Wei-qing, LIU Jing, HUANG Yang, FENG Qi-ming, ZHAO Hong. Fe(III) as an activator for the flotation of spodumene, albite, and quartz minerals [J]. Minerals Engineering, 2014, 61: 16−22.

[38] EJTEMAEI M, IRANNAJAD M, GHARABAGHI M. Role of dissolved mineral species in selective flotation of smithsonite from quartz using oleate as collector [J]. International Journal of Mineral Processing, 2012, 114: 40−47.

[39] WANG Yun-fan, K SULTAN A, LUO Xi-mei, TIAN Meng-jie. Understanding the depression mechanism of citric acid in sodium oleate flotation of Ca^{2+}-activated quartz: Experimental and DFT study [J]. Minerals Engineering, 2019, 140: 105878.

[40] FENG Qi-cheng, WEN Shu-ming, ZHAO Wen-juan, CHEN Hai-tao. Interaction mechanism of magnesium ions with cassiterite and quartz surfaces and its response to flotation separation [J]. Separation and Purification Technology, 2018, 206: 239−246.

[41] KOU J, XU S, SUN T, SUN C, GUO Y, WANG C. A study of sodium oleate adsorption on Ca^{2+} activated quartz surface using quartz crystal microbalance with dissipation [J]. International Journal of Mineral Processing, 2016, 154: 24−34.

[42] LIU Biao, WANG Xu-ming, DU Hao, LIU Jing, ZHENG Shi-li, ZHANG Yi, MILLER J D. The surface features of lead activation in amyl xanthate flotation of quartz [J]. International Journal of Mineral Processing, 2016, 151: 33−39.

[43] TIAN Meng-jie, LIU Run-qing, GAO Zhi-yong, CHEN Pan, HAN Hai-sheng, WANG Li, ZHANG Chen-yang, SUN Wei, HU Yue-hua. Activation mechanism of Fe (III) ions in cassiterite flotation with benzohydroxamic acid collector [J]. Minerals Engineering, 2018, 119: 31−37.

[44] TIAN Meng-jie, ZHANG Chen-yang, HAN Hai-sheng, LIU Run-qing, GAO Zhi-yong, CHEN Pan, WANG Li, LI Yun-zhi, JI Bin, HU Yue-hua, SUN Wei. Effects of the preassembly of benzohydroxamic acid with Fe (III) ions on its adsorption on cassiterite surface [J]. Minerals Engineering,

2018, 127: 32−41.

[45] TIAN Meng-jie, ZHANG Chen-yang, HAN Hai-sheng, LIU Run-qing, GAO Zhi-yong, CHEN Pan, HE Jian-yong, HU Yue-hua, SUN Wei, YUAN Dan-dan. Novel insights into adsorption mechanism of benzohydroxamic acid on lead (II)-activated cassiterite surface: An integrated experimental and computational study [J]. Minerals Engineering, 2018, 122: 327−338.

[46] TIAN Meng-jie, HU Yue-hua, SUN Wei, LIU Run-qing. Study on the mechanism and application of a novel collector-complexes in cassiterite flotation [J]. Colloids and Surfaces A: Physicochemical and Engineering Aspects, 2017, 522: 635−641.

[47] TRAHAR W J, SENIOR G D , HEYES G W, CREED M D. The activation of sphalerite by lead—A flotation perspective [J]. International Journal of Mineral Processing, 1997, 49: 121−148.

[48] V DUSICA R, PREDRAG M L, R ALEKSANDRA A. Ethyl xanthate adsorption and adsorption kinetics on lead-modified galena and sphalerite under flotation conditions [J]. Colloids and Surfaces A: Physicochemical and Engineering Aspects, 2006, 279: 96−104.

[49] WANG Han, WEN Shu-ming, HAN Guang, XU Lei, FENG Qi-cheng. Activation mechanism of lead ions in the flotation of sphalerite depressed with zinc sulfate [J]. Minerals Engineering, 2020, 146: 106132.

[50] DENG Rong-dong, HU Yuan, KU Jian-gang, ZUO Wei-ran, YANG Zheng-guo. Adsorption of Fe(III) on smithsonite surfaces and implications for flotation [J]. Colloids and Surfaces A: Physicochemical and Engineering Aspects, 2017, 533: 308−315.

[51] LIU Cheng, CHEN Yan-fei, SONG Shao-xian, LI Hong-qiang. The effect of aluminum ions on the flotation separation of pentlandite from lizardite [J]. Colloids and Surfaces A: Physicochemical and Engineering Aspects, 2018, 555: 708−712.

[52] RASHCHI F, SUI C, FINCH J A. Sphalerite activation and surface Pb ion concentration [J]. International Journal of Mineral Processing, 2002, 67: 43−58.

[53] RALSTON J, HEALY T W. Activation of zinc sulphide with CuII, CdII and PbII. I: Activation in weakly acidic media [J]. International Journal of Mineral Processing, 1980, 7: 175−201.

[54] RALSTON J, HEALY T W. Activation of zinc sulphide with CuII, CdII and PbII. II: Activation in neutral and weakly alkaline media [J]. International Journal of Mineral Processing, 1980, 7: 203−217.

[55] BOGUSZ E, BRIENNE S R, BUTLER I, RAO S R, FINCH J A. Metal ions and dextrin adsorption on pyrite [J]. Minerals Engineering, 1997, 10: 441−445.

[56] TIAN Meng-jie, HU Yue-hua, SUN Wei, LIU Run-qing. Study on the mechanism and application of a novel collector-complexes in cassiterite flotation [J]. Colloids and Surfaces A: Physicochemical and Engineering Aspects, 2017, 522: 635−641.

[57] TIAN Meng-jie, GAO Zhi-yong, SUN Wei, HAN Hai-sheng, SUN Lei, HU Yue-hua. Activation role of lead ions in benzohydroxamic acid flotation of oxide minerals: New perspective and new practice [J]. Journal of Colloid and Interface Science, 2018, 529: 150−160.

[58] TIAN Meng-jie, GAO Zhi-yong, KHOSO S A, SUN Wei, HU Yue-hua. Understanding the activation mechanism of Pb^{2+} ion in benzohydroxamic acid flotation of spodumene: Experimental findings and DFT simulations [J]. Minerals Engineering, 2019, 143: 106006.

[59] BULUT G, ATAK S. Role of dixanthogen on pyrite flotation: Solubility, adsorption studies and E_h, FTIR measurements [J]. Minerals & Metallurgical Processing, 2002, 19: 81−86.

[60] HAN Hai-sheng, HU Yue-hua, Sun Wei, LI Xiao-dong, CHEN Ke-feng, ZHU Yang-ge, NGUYEN A V, TIAN Meng-jie, WANG Li, YUE Tong, LIU Run-qing, GAO Zhi-yong, CHEN Pan, ZHANG Chen-yang, WANG Jian-jun, WEI Zhao, WANG Ruo-lin. Novel catalysis mechanisms of benzohydroxamic acid adsorption by lead ions and changes in the surface of scheelite particles [J]. Minerals Engineering, 2018, 119: 11−22.

[61] FANG Shuai, XU Long-hua, WU Hou-qin, SHU Kai-qian, XU Yan-bo, ZHANG Zhen-yue, CHI Ruan, SUN Wei. Comparative studies of flotation and adsorption of Pb(II)/benzohydroxamic acid collector complexes on ilmenite and titanaugite [J]. Powder Technology, 2019, 345: 35−42.

[62] FANG Shuai, XU Long-hua, WU Hou-qin, TIAN Jia, LU Zhong-yuan, SUN Wei, HU Yue-hua. Adsorption of Pb(II)/benzohydroxamic acid collector complexes for ilmenite flotation [J]. Minerals Engineering, 2018, 126: 16−23.

[63] CRUNDWELL F K. On the mechanism of the flotation of oxides and silicates [J]. Minerals Engineering, 2016, 95: 185−196.

[64] FUERSTENAU D W, PRADIP P. Zeta potentials in the flotation of oxide and silicate minerals [J]. Advances in Colloid and Interface Science, 2005, 114−115: 9−26.

[65] WANG Dian-zuo, HU Yue-hua. Solution chemistry of flotation [M]. Beijing: Science & Technology Press, 1988. (in Chinese)

[66] JAMES R O, HEALY T W. Adsorption of hydrolyzable metal ions at the oxide-water I: Co(ll) adsorption on SiO_2 and TiO_2 as model systems [J]. Journal of Colloid and Interface Science, 1971, 40: 41−52.

[67] OZKAN A, UCBEYIAY H, DUZYOL S. Comparison of stages in oil agglomeration process of quartz with sodium oleate in the presence of Ca(II) and Mg(II) ions [J]. Journal of Colloid and Interface Science, 2009, 329: 81−88.

[68] BURDUKOVA E, van LEERDAM G C, PRINS F E, SMEINK R G, BRADSHAW D J, LASKOWSKI J S. Effect of calcium ions on the adsorption of CMC onto the basal planes of New York talc: A ToF-SIMS study [J]. Minerals Engineering, 2008, 21: 1020−1025.

[69] JIN Sai-zhen, SHI Qing, FENG Qi-ming, ZHANG Guo-fan, CHANG Zi-yong. The role of calcium and carbonate ions in the separation of pyrite and talc [J]. Minerals Engineering, 2018, 119: 205−211.

[70] LIU Wei-jun, ZHANG Shi-qiu, WANG Wei-qing, ZHANG Jie, YAN Wu, DENG Jie, FENG Qi-ming, HUANG Yang. The effects of Ca(II) and Mg(II) ions on the flotation of spodumene using NaOL [J]. Minerals Engineering, 2015, 79: 40−46.

[71] ZHU Guang-li, WANG Yu-hua, WANG Xu-ming, MILLER J D, LU Dong-fang, ZHANG Xia-yu, ZHAO Yue-hao, ZHENG Hai-tao. Effects of grinding environment and lattice impurities on spodumene flotation [J]. Transactions of Nonferrous Metals Society of China, 2019, 29: 1527−1537.

[72] LI Hong-qiang, MU Shun-xing, WENG Xiao-qing, ZHAO Yun-liang, SONG Shao-xian. Rutile flotation with Pb^{2+} ions as activator: Adsorption of Pb^{2+} at rutile/water interface [J]. Colloids and Surfaces A: Physicochemical and Engineering Aspects, 2016, 506: 431−437.

[73] CAO Miao, GAO Yu-de, BU Hao, QIU Xian-yang. Study on the mechanism and application of rutile flotation with benzohydroxamic acid [J]. Minerals Engineering, 2019, 134: 275−280.

[74] FUERSTENAU M C, MARTIN C C, BHAPPU R B. The role of hydrolysis in sulfonate flotation of quartz [J]. Society of Mining Engineers, 1963, 226: 449−454.

[75] FUERSTENAU M C, BHAPPU R B. Sulfonate flotation of beryl [M]. New Mexico Bureau of Mines, 1963.

[76] TIAN Meng-jie, GAO Zhi-yong, HAN Hai-sheng, SUN Wei, HU Yue-hua. Improved flotation separation of cassiterite from calcite using a mixture of lead (II) ion/ benzohydroxamic acid as collector and carboxymethyl cellulose as depressant [J]. Minerals Engineering, 2017, 113: 68−70.

[77] MIELCZARSKI J. The role of impurities of sphalerite in the adsorption of ethyl xanthate and its flotation [J]. International Journal of Mineral Processing, 1986, 16(3): 179−194.

[78] MOSLEMI H, GHARABAGHI M. A review on electrochemical behavior of pyrite in the froth flotation process [J]. Journal of Industrial and Engineering Chemistry, 2017, 47: 1−18.

[79] BERTIL P, ERIC K S. Computer-assisted calculations of thermodynamic equilibria in sphalerite-xanthate systems [J]. International Journal of Mineral Processing, 1989, 26: 223−258.

[80] BERTIL P, ERIC K S. Computer-assisted calculations of thermodynamic equilibria in the galena−ethyl xanthate system [J]. International Journal of Mineral Processing, 1988, 23: 93−121.

[81] WANG Xiang-huai, ERIC F, BOLIN J. Thermodynamic calculations on iron-containing sulphide mineral flotation systems, I. The stability of iron-xanthates [J]. International Journal of Mineral Processing, 1989, 27: 1−19.

[82] LASKOWSKI J S, LIU Q, ZHAN Y. Sphalerite activation: Flotation and electrokinetic studies [J]. Minerals Engineering, 1997, 10: 787−802.

[83] WANG Xiang-huai, ERIC F, NILS J B. The aqueous and surface chemistry of activation in the flotation of sulphide minerals—A review. Part II: A surface precipitation model [J]. Mineral Processing and Extractive Metallurgy Review, 1989, 4: 167−199.

[84] WANG Xiang-huai, ERIC F, NILS J B. The aqueous and surface chemistry of activation in the flotation of sulphide minerals—A review. Part I: An electrochemical model [J]. Mineral Processing and Extractive Metallurgy Review, 1989, 4: 135−165.

[85] FINKELSTEIN N P. The activation of sulphide minerals for flotation: A review [J]. International Journal of Mineral Processing, 1997, 52: 81−120.

[86] CHANDRA A P, GERSON A R. A review of the fundamental studies of the copper activation mechanisms for selective flotation of the sulfide minerals, sphalerite and pyrite [J]. Advances in Colloid and Interface Science, 2009, 145: 97−110.

[87] GERSON A R, LANGE A G , PRINCE K E , SMART R C. The mechanism of copper activation of sphalerite [J]. Applied Surface Science, 1999, 137: 207−223.

[88] KARTIO I J, BASILIO C I, YOON R H. An XPS study of sphalerite activation by copper [J]. Langmuir, 1998, 14: 5274−5278.

[89] PATTRICK R A, ENGLAND K E, CHARNOCK J M, MOSSELMANS J F. Copper activation of sphalerite and its reaction with xanthate in relation to flotation: An X-ray absorption spectroscopy (reflection extended X-ray absorption fine structure) investigation [J]. International Journal of Mineral Processing, 1999, 55: 247−265.

[90] BUCKLEY A N, SKINNER W M, L HARMER S, PRING A, LAMB R N, FAN Liang-jen, YANG Yaw-wen. Examination of the proposition that Cu(II) can be required for charge neutrality in a sulfide lattice: Cu in tetrahedrites and sphalerite [J]. Canadian Journal of Chemistry, 2007, 85: 767−781.

[91] PAROLIS L A, RENE V M, GROENMEYER G V, HARRIS P J. The influence of metal cations on the behaviour of carboxymethyl celluloses as talc depressants [J]. Colloids and Surfaces A: Physicochemical and Engineering Aspects, 2008, 317: 109−115.

[92] JIN Sai-zhen, SHI Qing, LI Qi, OU Le-ming, OUYANG Kai. Effect of calcium ionic concentrations on the adsorption of carboxymethyl cellulose onto talc surface: Flotation, adsorption and AFM imaging study [J]. Powder Technology, 2018, 331: 155−161.

[93] YU Li, LIU Quan-jun, LI Shi-mei, DENG Jiu-shuai, LUO Bin, LAI Hao. Adsorption performance of copper ions on arsenopyrite surfaces and implications for flotation [J]. Applied Surface Science, 2019, 488: 185−193.

[94] ZHAO Wen-juan, LIU Dian-wen, WEN Shu-ming, FENG Qi-cheng. Surface modification of hemimorphite with lead ions and its effect on flotation and oleate adsorption [J]. Applied Surface Science, 2019, 483: 849−858.

[95] WANG Ji-zhen, MAO Yong, CHENG Ya-zhi, XIAO Yu-chen, ZHANG Yu-xuan, BAI Jun-zhi. Effect of Pb(II) on the flotation behavior of scheelite using sodium oleate as collector [J]. Minerals Engineering, 2019, 136: 161−167.

[96] GAO Yue-sheng, JUNG S, PAN Lei. Interaction and instability of air films between bituminous coal surfaces and surfactant droplets [J]. Fuel, 2020, 274: 117839.

[97] YATES D E, HEALY T W. Titanium dioxide–electrolyte interface. Part 2: Surface charge (titration) studies [J]. Journal of the Chemical Society, Faraday Transactions 1: Physical Chemistry in Condensed Phases, 1980, 76: 9−18.

[98] HUANG Zi-jie, WANG Jian-jun, SUN Wei, HU Yue-hua, CAO Jian, GAO Zhi-yong. Selective flotation of chalcopyrite from pyrite using diphosphonic acid as collector [J]. Minerals Engineering, 2019, 140: 105890.

[99] REN Liu-yi, HANG Qiu, ZHANG Yi-min, NGUYEN A V, ZHANG Ming, WEI Peng-gang, LONG Qiu-rong. Effects of alkyl ether amine and calcium ions on fine quartz flotation and its guidance for upgrading vanadium from stone coal [J]. Powder Technology, 2018, 338: 180−189.
[100] FENG Qi-cheng, WEN Shu-ming, ZHAO Wen-juan, CHEN Yu. Effect of calcium ions on adsorption of sodium oleate onto cassiterite and quartz surfaces and implications for their flotation separation [J]. Separation and Purification Technology, 2018, 200: 300−306.
[101] ZHAO Qiang, LIU Wen-gang, WEI De-zhou, WANG Wen-dan, CUI Bao-yu, LIU Wen-bao. Effect of copper ions on the flotation separation of chalcopyrite and molybdenite using sodium sulfide as a depressant [J]. Minerals Engineering, 2018, 115: 44−52.
[102] FENG Qi-cheng, ZHAO Wen-juan, WEN Shu-ming, CAO Qin-bo. Activation mechanism of lead ions in cassiterite flotation with salicylhydroxamic acid as collector [J]. Separation and Purification Technology, 2017, 178: 193−199.
[103] DONG Liu-yang, JIAO Fen, QIN Wen-qing, ZHU Hai-ling, JIA Wen-hao. Activation effect of lead ions on scheelite flotation: Adsorption mechanism, AFM imaging and adsorption model [J]. Separation and Purification Technology, 2019, 209: 955−963.
[104] HUNTER R J. Zeta potential in colloid science: Principles and application [M]. London: Academic Press, 2013.
[105] SONG Chao, ZHOU Yuan-yuan, LIU Quan-jun, DENG Jian-ying, LI Shi-mei, GAO Li-kun, YU Li. Effects of $BaCl_2$ on K-feldspar flotation using dodecyl amine chloride under natural pH [J]. Transactions of Nonferrous Metals Society of China, 2018, 28: 2335−2341.
[106] YANG Bing-qiao, WANG De-ru, WANG Tian-shuai, ZHANG Han-quan, JIA Fei-fei, SONG Shao-xian. Effect of Cu^{2+} and Fe^{3+} on the depression of molybdenite in flotation [J]. Minerals Engineering, 2019, 130: 101−109.
[107] WANG Jian-jun, LI Wen-heng, ZHOU Zi-han, GAO Zhi-yong, HU Yue-hua, SUN Wei. 1-Hydroxyethylidene-1, 1-diphosphonic acid used as pH-dependent switch to depress and activate fluorite flotation I: Depressing behavior and mechanism [J]. Chemical Engineering Science, 2020, 214: 115369.
[108] MCDONALD S, ELBOURNE A, WARR G G, ATKIN R. Metal ion adsorption at the ionic liquid-mica interface [J]. Nanoscale, 2016, 8: 906−914.
[109] LIU Wei-jun, ZHANG Shi-qiu, WANG Wei-qing, ZHANG Jie, YAN Wu, DENG Jie, FENG Qi-ming, HUANG Yang. The effects of Ca(II) and Mg(II) ions on the flotation of spodumene using NaOL [J]. Minerals Engineering, 2015, 79: 40−46.
[110] CHEN Pan, ZHAI Ji-hua, SUN Wei, HU Yue-hua, YIN Zhi-gang, LAI Xiang-sheng. Adsorption mechanism of lead ions at ilmenite water interface and its influence on ilmenite flotability [J]. Journal of Industrial and Engineering Chemistry, 2017, 53: 285−293.
[111] YU Fu-shun, WANG Yu-hua, WANG Jin-ming, XIE Zhen-fu, ZHANG Lei. First-principle investigation on mechanism of Ca ion activating flotation of spodumene [J]. Rare Metals, 2014, 33: 358−362.
[112] LIU Jian, WEN Shu-ming, DENG Jiu-shuai, CHEN Xiu-min, FENG Qi-cheng. DFT study of ethyl xanthate interaction with sphalerite (110) surface in the absence and presence of copper [J]. Applied Surface Science, 2014, 311: 258−263.
[113] CHEN Zhuo, YOON R H. Electrochemistry of copper activation of sphalerite at pH 9.2 [J]. International Journal of Mineral Processing, 2000, 58: 57−66.

金属离子在矿物浮选中的典型作用

高志勇[1,2]，江哲伊[1,2]，孙 伟[1,2]，高跃升[3]

1. 中南大学 资源加工与生物工程学院，长沙 410083；
2. 中南大学 战略含钙矿物资源清洁高效利用湖南省重点实验室，长沙 410083；
3. Department of Chemical Engineering, Michigan Technological University, Houghton 49931, United States

摘 要：在矿物浮选中，金属离子可以通过选择性活化或抑制矿物表面，从而发挥重要的作用。尽管此前大量工作报道了金属离子在浮选中的作用，但大多仅是针对某一特定类型金属离子或目的矿物进行研究分析，缺乏一个全面的综述。本文对金属离子在矿物浮选中的影响因素进行详细分类，总结金属离子在不同种类矿物浮选中的作用机理。此外，还对常见探索作用机理的研究方法，包括经典的浮选、接触角测量、动电位测量，以及近年来流行的模拟计算、溶液化学计算和循环伏安等，进行梳理和分析。本文全面综述了金属离子在矿物浮选中的作用，发现金属离子的添加与去除、溶液化学环境改变、浮选药剂的选择等都可调控金属离子对矿物浮选的影响，对于精确调控矿物浮选具有重要指导意义。

关键词：金属离子；浮选；氧化矿；硅酸盐矿；硫化矿

(Edited by Xiang-qun LI)